STRUCTURE OF ACTIVATED CARBONS PRODUCED FROM PAPER MILL SLUDGE USING SMALL ANGLE NEUTRON SCATTERING

[1]Giselle Sandí*, [2]Nasrin R. Khalili, [3]Kenneth C. Littrell, and [3]P. Thiyagarajan

[1]Chemistry and [3]Intense Pulsed Neutron Source Divisions, Argonne National Laboratory, 9700 South Cass Ave., Argonne, IL 60439; [2]Department of Chemical and Environmental Engineering, Illinois Institute of Technology, Chicago, Illinois 60616

ABSTRACT

A novel, cost-effective, and environmentally benign process was developed to produce highly efficient carbon-based adsorbents (CBAs) from paper mill sludge. The production process required chemical activation of sludge using zinc chloride and pyrolysis at 750°C in N_2 gas. The produced CBAs were characterized according to their surface area and pore size distribution using N_2-BET adsorption isotherm data. Further characterization of the surface and pore structure was conducted using small angle neutron scattering (SANS). The structural features analyzed by SANS revealed the dependence of porosity on zinc chloride concentration. The presence of inaccessible pores was also determined by solvent contrast-variation SANS experiments.

KEYWORDS: SANS, carbon-based adsorbents, paper mill sludge, porosity.

INTRODUCTION

A series of novel carbon-based adsorbents (CBAs) have been produced from paper mill sludge. The significant feature of the produced sludge-based activated carbon, that makes it a unique and particularly economical adsorbent/catalyst/catalyst support system, is that waste materials are used for its production. The produced CBAs can be extensively used as adsorbents, catalysts and catalyst supports in a variety of industrial and environmental applications (such as purification processes, recovery of chemical products, and removal of organic and metals). Their adsorption capability and catalytic activity are largely controlled by their surface characteristics [1,2]. For example, carbons used for the adsorption of gases and vapors should have pores with effective radii considerably smaller than 16-20 Å [2], while activated carbons with pore sizes in the range of 20-500 Å have been shown to be significant adsorbents for the removal of coloring impurities from liquid phase systems [3]. The relationship between the surface properties of activated carbon and its effectiveness as an adsorbent or catalyst, emphasizes the importance of developing methodologies by which activated carbon with specified surface properties can be produced.

Analysis of the surface physical properties of the produced carbons initially included determination of the total surface area, extent of microporosity, and characterization of the pore size distribution using nitrogen adsorption isotherms data [2, 3, 4]. While the results of the surface analysis have shown that activation methodology used to produce novel CBAs has a significant impact on the surface structure and performance of the carbons produced, these data alone were not sufficient to draw definite conclusions about the extent of correlation between the carbons' microporous structure and the activation methodologies employed in their production. Therefore, small angle neutron scattering (SANS) was used to supplement existing analysis and provide valuable information about the microscopic structures of the carbons produced. such as produced pore distribution, pore width, pore radii, characteristic lengths, and voids. The SANS data were used to study the surface properties of the carbons at mesoscopic length scales and to characterize their microstructure by determining the sizes and geometries of the component clusters and through solvent contrast variation, the accessibility of their micropores to solvent.

This information is fundamental for the characterization of these carbons and evaluation of the extent of availability of their pores to adsorbates in gas and/or liquid phase environments.

EXPERIMENTAL

The raw paper mill sludge was first dried in an oven at 110°C for 24 hours, then crushed mechanically using a paint-mixing machine. Crushing provided smaller particles with increased surface area and also enabled more efficient chemical activation of the raw material. Samples were sieved after mechanical crushing to obtain particle with sizes smaller than 600 μm. This particle size range was found to be the most suitable for the chemical activation process that was performed using five different $ZnCl_2$ to dried sludge mass ratios of 0.75, 1.0, 1.5, 2.0, and 2.5 [5]. To ensure a complete reaction between $ZnCl_2$ and sludge particles, sludge was mixed with zinc chloride at 85°C for 7 hours. After chemical activation, samples were dried in air at 110°C for 24-36 hours. The time required for drying varied depending on the amount of zinc chloride used for the activation process (i.e., higher impregnation ratios required longer drying time). After drying, the sludge was crushed again into a fine powder. Chemically activated samples were exposed to light and humidity (L&H) for about 22 hours to enhance the development of the pore structure during pyrolysis [5].

Pyrolysis of the chemically activated and L&H-treated sludge was carried out in an inert environment (70ml/min flow of nitrogen gas) at 800°C for two hours. Upon completion of the pyrolysis, the sample was removed from the reactor and crushed using a mortar and a pestle. The crushed samples were then cleansed using 500 ml of 1.2 M HCl followed by 500 mL of distilled water to remove excess zinc chloride and residual inorganic matter. After drying in air, the samples were transferred to 20-mL vials for storage prior to conducting the physical activation process. During the physical activation, samples were heated for two hours at 800 °C in a mixture of 75% CO and 25% CO_2. Upon completion of the physical activation, the produced carbons were characterized according to their surface properties by BET and related measurements.

For the SANS measurements, the carbons were ground into a powder. The SANS measurements at the SAND time-of-flight SANS instruments at the Intense Pulsed Neutron Source at Argonne National Laboratory [6] using cylindrical Suprasil sample containers with a neutron optical path length of 1 mm. SAND provides data in a Q range of 0.004 to 0.6 Å^{-1} in a single measurement. All samples were studied as dry powders. Additionally, a contrast-variation SANS study was performed on the sample treated with the highest zinc chloride ratio by preparing the powdered sample as slurries in mixtures of normal and deuterated toluene with deuterated toluene proportions of 0, 25, 50, 75 and 100 %. In preparing the slurries, the powder was slowly evacuated to avoid air bubble formation prior to adding the solvent. The scattering from an empty cell was used for background correction in these measurements.

RESULTS AND DISCUSSION

The SANS data for the dry powder samples was initially analyzed by using a modified version of the unified Guinier analysis and power law model proposed by Beaucage et al. [7, 8] to fit the full range of the data. As shown in Table 1, the results of this unified fit indicate that at the lowest Q scale, the behavior all of the dry powder carbon samples except the one prepare with a 0.75/1 $ZnCl_2$ ratio is that of surface-fractal interfaces of large objects. However, the low Q fractal dimension of –4 obtained for the 0.75/1 $ZnCl_2$ ratio sample is characteristic of a smooth interface. At higher Q and thus shorter length scales, the power law exponents obtained were consistent with those from mass fractal aggregates.

In order to gain a better understanding of the microstructure of these systems, we subtracted the low-Q power law behavior from the measured scattering curves, enhancing the visibility of features at higher Q, and fit the difference data using the model developed by Teixiera [9]. In this model, which describes the scattering from mass fractal aggregates of small, uniform spheres of radius R, the scattered intensity is given by:

$$I(Q;\xi,D_F,R) = I_{0S}\left(1 + \frac{\sin[(D_F-1)\arctan(Q\xi)]}{(QR)^{D_F}\left(\dfrac{1}{Q^2\xi^2}+1\right)^{\frac{D_F-1}{2}}}\right)P_{Sphere}(Q;R) + I_{Background}$$

where D_F is the mass-fractal dimension, ξ is the exponential cutoff length for the aggregate, $I_{Background}$ is the background intensity, and I_{0S} is the intensity scattered by the fundamental sphere extrapolated to $Q=0$. Here,

$$P_{Sphere}(Q,R) = \left[\frac{3(\sin(QR)-QR\cos(QR))}{(QR)^3}\right]^2$$

is the scattering form factor for the fundamental sphere [10].

The data with the low Q power law scattering subtracted is compared with the fit functions in figure 1 and the corresponding fit parameters are given in Table1. The results of the Teixeira model fits to the data for the samples prepared with the three highest ratios of $ZnCl_2$ indicates that these samples are similar in their microstructure. For these samples, both the fractal dimension and the size of the aggregates as indicated by the exponential cutoff size parameter ξ increase as the $ZnCl_2$ ratio increases. However, the other two samples are significantly different in their microstructure. The sample prepared with a $ZnCl_2$ ratio of 0.75 has a much lower mass fractal dimension and a much larger extent. The sample prepared with a $ZnCl_2$ ratio of 1.0 has a mass fractal dimension close to 1 and is better fit by the form factor for a cylinder [10]. Similar behavior has also been observed in silica systems [11]. The size of the fundamental particle of which these aggregates are composed is found from the fits to be approximately 2 Å and is thus of nearly atomic size.

The same approach was used to analyze the data from the solvent contrast variation study performed using slurries of the sample with a $ZnCl_2$ ratio of 2.5 immersed in different mixtures of toluene and deuterated toluene. The results of the fits are presented in Table 2. The quality of the fits to the data with the low Q power law behavior subtracted is shown in figure 2. The low-Q power law of this sample in 100% D-toluene was that of a mass fractal while all of the other samples had surface-fractal power-laws. Similarly, while the other four samples were well described by the Teixeira mass fractal model at high Q, the data for the sample in 100% deuterated toluene is inconsistent with this model but well described as a polydisperse, nearly hollow shell. The change in the shapes of the scattering curves without loss of intensity at low Q seen in figure 2 for the three samples with the highest concentration of deuterated toluene indicates that the toluene solvent is unable to completely contrast-match the scattering length density of the aggregates. This suggests that the toluene is not able to completely penetrate the micropores in these samples.

CONCLUSIONS

This SANS study has shown that the microscopic structure of these activated carbons prepared from paper-mill sludge is sensitively dependent on the ratio of $ZnCl_2$ used in their preparation. The mass fractal dimensions observed for the samples prepared with higher ratios of $ZnCl_2$ are similar to each other and to the fractal dimension of 2.5 associated with growth by percolation and/or diffusion-limited aggregation. The parallel trends observed in BET analysis and the structural determination by small angle scattering for these samples shows that modifications of the production procedure can significantly and systematically alter the quality and characteristics of the final products. The lower fractal dimensions of the other two samples show that they are lower dimensional structures. The fitted fractal dimension was consistent with the rod-like structure observed for the sample prepared with $ZnCl_2$/sludge ratio of 1.

The small pore structure of these carbons suggests that they can be used in a variety of gas-phase cleaning applications. Further studies of the catalytic and adsorbate properties of these activated carbons and others similar to them correlated with these studies of their microstructure and mesoscopic surface structure will allow for the production procedure to be systematically tailored to produce activated carbons that are optimized for performance in a variety of applications.

ACKNOWLEDGMENTS

REFERENCES

[1]   Bansal, R. C.; Donnet, J.; Stoeckli, F. *Active Carbon*, NY:New York City, **1988**.

[2]   Boppart, S.; Ingle, L.; Potwora, R. J.; Rester, D. O. *Chemical Processing* **1996**, 79.

[3]   Walker, P. L. *Chemistry and Physics of Carbon*, NY:New York City, **1996**.

[4]   Campbell, M. MS thesis, Illinois Institute of Technology, **1998**.

[5]   Khalili, N. R. IIT Patent #147, **1999**.

[6]   Thiyagarajan, P.; Epperson, J. E.; Crawford, R. K.; Carpenter, J. M.; Klippert, T. E; Wozniak.; D. G. *J. Appl. Cryst.* **1997**, *30*, 280.

[7]   Beaucage, G. *J. Appl. Cryst.* **1996**, *29*, 134.

[8]   Beaucage, G. *J. Appl. Cryst.***1995**, *26*, 717.

[9]   Teixeira, J. J. Appl. Cryst. **1988**, *21*, 781.

[10]   Pedersen, J. S. *Adv. Colloid Interface Sci.*, **1997**, *70*, 171.

[11]   Hyeon-Lee, J.; Beaucage, G.; Pratsinis, S. E. *Chem. Mater.* **1997**, *9*, 2400.
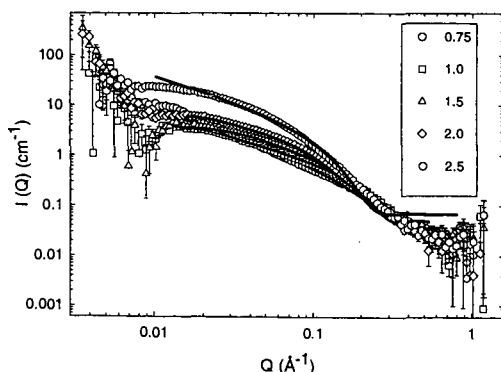
Figure 1: Resulting SANS plots after subtraction of the low Q power law. The solid lines indicate the fit to the Teixeira model.

Table I: Results of the Teixeira sphere mass fractal fit to the samples shown in figure 1.

ZnCl$_2$/sludge ratio	BET surface area (m^2/g)	Low Q Power Law Exponent	High Q Fractal dimension	Cutoff Length ξ (Å)
0.75	895	-4.02 ± 0.04	1.37 ± 0.01	NA (too large)
1.0*	1015	-3.46 ± 0.02	1.19 ± 0.02	67 ± 4
1.5	1067	-3.59 ± 0.01	2.18 ± 0.02	15.6 ± 0.3
2.0	1095	-3.70 ± 0.01	2.36 ± 0.02	17.2 ± 0.2
2.5	1249	-3.52 ± 0.02	2.50 ± 0.01	23.4 ± 0.2

* This data set was better fit by the form factor for a cylinder of radius 7.84 ± 0.09 Å and length 179.6 ± 4.8 Å.
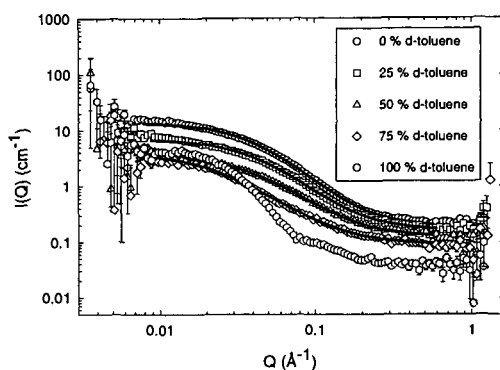

Figure 2: SANS plots of ZnCl$_2$/sludge ratio of 2.5, immersed in different toluene/d-toluene mixtures.

Table II: Results of the Teixeira sphere mass fractal fit to the samples shown in figure 2.

2.5 ZnCl$_2$/sludge ratio Sample in	Low Q Power Law Exponent	High Q Fractal dimension	Cutoff Length ξ (Å)
0 % d-toluene	-3.64 ± 0.03	2.42 ± 0.01	23.6 ± 0.2
25 % d-toluene	-3.70 ± 0.06	2.35 ± 0.02	22.6 ± 0.4
50 % d-toluene	-3.67 ± 0.11	2.26 ± 0.03	23.1 ± 0.7
75 % d-toluene	-3.29 ± 0.11	2.03 ± 0.04	46.5 ± 2.1
100 % d-toluene	-2.82 ± 0.04	NA	NA